Vertical density matrix algorithm: A higher-dimensional numerical renormalization scheme based on the tensor product state ansatz

Nobuya Maeshima,[1] Yasuhiro Hieida,[2] Yasuhiro Akutsu,[1] Tomotoshi Nishino,[2] and Kouichi Okunishi[3]
[1]*Department of Physics, Graduate School of Science, Osaka University, Toyonaka 560-0043, Japan*
[2]*Department of Physics, Graduate School of Science, Kobe University, Rokkoudai 657-8501, Japan*
[3]*Department of Physics, Faculty of Science, Niigata University, Igarashi 950-2181, Japan*
(Received 23 January 2001; published 26 June 2001)

We present a new algorithm to calculate the thermodynamic quantities of three-dimensional (3D) classical statistical systems, based on the ideas of the tensor product state and the density matrix renormalization group. We represent the maximum-eigenvalue eigenstate of the transfer matrix as the product of local tensors that are iteratively optimized by the use of the ''vertical density matrix'' formed by cutting the system along the transfer direction. This algorithm, which we call *vertical density matrix algorithm* (VDMA), is successfully applied to the 3D Ising model. Using the Suzuki-Trotter transformation, we can also apply the VDMA to 2D quantum systems, which we demonstrate for the 2D transverse field Ising model.

DOI: 10.1103/PhysRevE.64.016705 PACS number(s): 02.70.−c, 05.10.Cc, 05.50.+q, 64.60.Cn

I. INTRODUCTION

Since the density matrix renormalization group (DMRG) method was invented by White [1], the method has been applied to various problems in one-dimensional (1D) quantum systems and 2D classical systems [2]. Such a great success of the DMRG has been stimulating us to extend the algorithm to the one that can handle higher-dimensional systems, principally 2D quantum systems and 3D classical systems [3–6].

We should recall that, in the DMRG, the matrix-product structure of the wave function of the target states (usually the ground state or the maximum-eigenvalue eigenstate) is essential [7]. From this point of view, the tensor-product state (TPS), which is a natural higher-dimensional generalization of the matrix product state, should play a key role in the ''higher-dimensional DMRG.'' A simple but nontrivial example of the TPS is the ground state of 2D valence-bond-solid (VBS)-type quantum spin systems, where the wave function is expressed as a product of local finite-dimensional tensors with all the tensor indices being contracted [8]. As for 3D classical statistical systems, the maximum-eigenvalue eigenstate of the layer-to-layer transfer matrix of the 3D classical system can exactly be represented as the TPS, if we allow the tensor dimension to be infinite. We should note that we can reduce the calculation of the expectation value of the TPS to a statistical average in a lower-dimensional classical system; a $(D+1)$-dimensional classical (or D-dimensional quantum) problem reduces to a D-dimensional classical statistical problem [9]. In fact, the properties of the 2D VBS model have been studied in terms of a 2D vertex model associated with the TPS wave function [9,10].

When developing the TPS formulation, the most important step is the determination (optimization) of the local tensor in the TPS. In Refs. [11,12], direct variational formulations are employed for the optimization of the local tensors. As compared with these ''direct'' methods, our algorithm given in the present paper for 3D classical systems is more like the original DMRG. The local tensor is updated by the ''block-spin basis transformation'' along the vertical direction. Since this transformation is constructed in terms of the density matrix made along the ''vertical direction'' (transfer direction of the transfer matrix), we call this algorithm the *vertical density matrix algorithm* (VDMA). We apply the VDMA to the 3D Ising model and discuss its efficiency. We also report the application of the VDMA to the 2D transverse field Ising model, with help of the Suzuki-Trotter transformation [13].

This paper is organized as follows. In Sec. II, we briefly explain the VDMA for 3D classical spin systems taking the 3D Ising model as an example. In Sec. III we show the numerical result for the 3D Ising model and the 2D transverse field Ising model. The last section is devoted to the conclusion.

II. METHOD

Let us consider the 3D Ising model on the simple cubic lattice of the size $N\times N\times 2L$ in X, Y, and Z directions. Suppose that L and N are sufficiently large and the neighboring Ising spins σ and σ' have ferromagnetic interaction $-J\sigma\sigma'$. Then the Boltzmann weight for the unit cube is written as

$$W\begin{pmatrix} \overline{\sigma}_{ij} & \overline{\sigma}_{i'j} & \overline{\sigma}_{i'j'} & \overline{\sigma}_{ij'} \\ \sigma_{ij} & \sigma_{i'j} & \sigma_{i'j'} & \sigma_{ij'} \end{pmatrix} \equiv \exp\Bigg[-\frac{K}{2}\big(\sigma_{ij}\sigma_{i'j}+\sigma_{i'j}\sigma_{i'j'} + \sigma_{i'j'}\sigma_{ij'}+\sigma_{ij'}\sigma_{ij}+\overline{\sigma}_{ij}\overline{\sigma}_{i'j} + \overline{\sigma}_{i'j}\overline{\sigma}_{i'j'}+\overline{\sigma}_{i'j'}\overline{\sigma}_{ij'} + \overline{\sigma}_{ij'}\overline{\sigma}_{ij}+\sigma_{ij}\overline{\sigma}_{ij}+\sigma_{i'j}\overline{\sigma}_{i'j} + \sigma_{i'j'}\overline{\sigma}_{i'j'}+\sigma_{ij'}\overline{\sigma}_{ij'}\big)\Bigg], \quad (1)$$

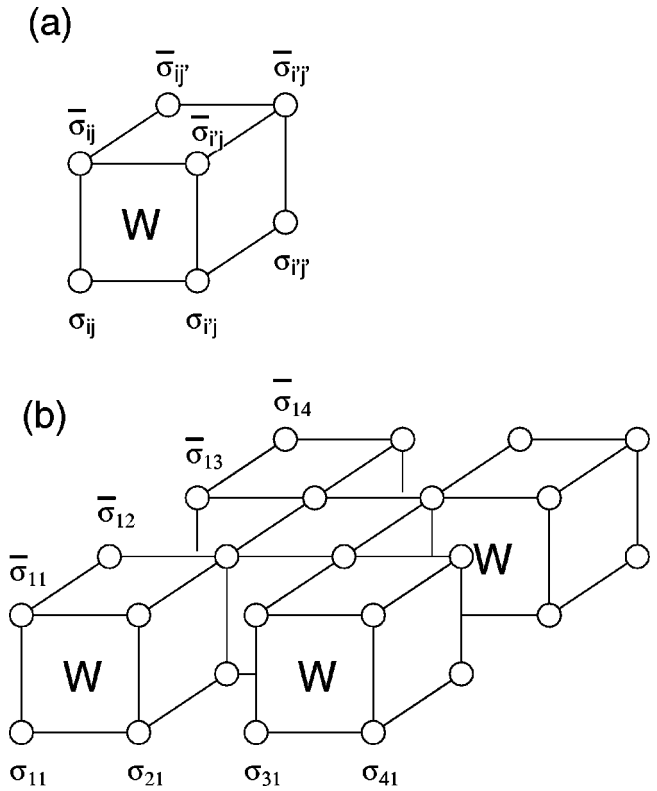

FIG. 1. (a) The Boltzmann weight of a unit cell and (b) the transfer matrix $T[\bar{\Omega}|\Omega]$ $(N=4)$.

where $i'=i+1$, $j'=j+1$, and $K=J/T$. The locations of the spin variables are shown in Fig. 1(a).

For the book keeping, let us introduce here some notations for spin variables. Write the configuration of the four spins surrounding a plaquette in the XY plane as

$$\boldsymbol{\sigma}_{ij}=(\sigma_{ij}\sigma_{i'j}\sigma_{i'j'}\sigma_{ij'}), \tag{2}$$

where the position of the plaquette can be labeled by the index ij. Then the Boltzmann weight is simply written as $W\left(\begin{smallmatrix}\boldsymbol{\sigma}_{ij}\\ \boldsymbol{\sigma}_{ij}\end{smallmatrix}\right)$. Also for a spin layer in the XY plane, we denote the configuration of the $N\times N$ spins as

$$[\Omega]\equiv\begin{bmatrix}\sigma_{11} & \cdots & \sigma_{1N}\\ \vdots & \ddots & \vdots\\ \sigma_{N1} & \cdots & \sigma_{NN}\end{bmatrix}. \tag{3}$$

Using these notations, the transfer matrix T from a layer $[\Omega]$ to the next layer $[\bar{\Omega}]$ is written as

$$T[\bar{\Omega}|\Omega]=\prod_{i+j=even} W\begin{pmatrix}\bar{\boldsymbol{\sigma}}_{ij}\\ \boldsymbol{\sigma}_{ij}\end{pmatrix}. \tag{4}$$

In the product of Eq. (4), the spin variables are shared by the adjacent cubes in the diagonal direction and thus the Boltzmann weights form the checkerboard pattern in the XY plane [see Fig. 1(b)].

Our goal is to evaluate the maximum eigenvalue $\lambda_{\max}$ of the transfer matrix T and the corresponding eigenvector

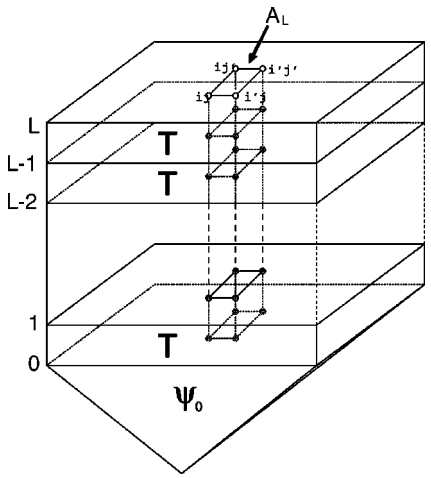

FIG. 2. The graphical representation of the vector $|\psi_L\rangle$. Below the ij plaquette, we find that the L unit cubes are piling up.

$|\psi_{\max}\rangle$, using the TPS representation of the eigenvector. In order to analyze the TPS structure of $|\psi_{\max}\rangle$, let us consider the power method briefly, which is the simplest but powerful technique to calculate $\lambda_{\max}$ and $|\psi_{\max}\rangle$. Define the vector $|\psi_L\rangle$ as

$$|\psi_L\rangle=T^L|\psi_0\rangle, \tag{5}$$

where $|\psi_0\rangle$ is an ''initial'' vector that is not orthogonal to $|\psi_{\max}\rangle$. Then the maximum-eigenvalue eigenvector $|\psi_{\max}\rangle$ is obtained as

$$|\psi_{\max}\rangle=\text{const}\times\lim_{L\to\infty}|\psi_L\rangle. \tag{6}$$

In Fig. 2, we show the graphical representation of $|\psi_L\rangle$, where we can see the structure of $|\psi_L\rangle$ more clearly. As is seen in this figure, the L unit cubes are piling vertically up to the surface, and then the product of the vertically arranged Boltzmann weights can be regarded as a local tensor; we define the local tensor A_L at the ij plaquette as

$$A_L\begin{pmatrix}\boldsymbol{\sigma}_{ij}^L\\ \boldsymbol{\xi}_{ij}^L\end{pmatrix}=W\begin{pmatrix}\boldsymbol{\sigma}_{ij}^L\\ \boldsymbol{\sigma}_{ij}^{L-1}\end{pmatrix}W\begin{pmatrix}\boldsymbol{\sigma}_{ij}^{L-1}\\ \boldsymbol{\sigma}_{ij}^{L-2}\end{pmatrix}\cdots W\begin{pmatrix}\boldsymbol{\sigma}_{ij}^{1}\\ \boldsymbol{\sigma}_{ij}^{0}\end{pmatrix}, \tag{7}$$

where $\boldsymbol{\sigma}_{ij}^L$ is the spin configuration at the ij plaquette on the ''surface layer,'' and the auxiliary variable $\boldsymbol{\xi}_{ij}^L\equiv(\boldsymbol{\sigma}_{ij}^0\boldsymbol{\sigma}_{ij}^1\boldsymbol{\sigma}_{ij}^2\cdots\boldsymbol{\sigma}_{ij}^{L-1})$ denotes the configuration for the spins under the surface. Using the local tensors defined above, $|\psi_L\rangle$ is represented as a TPS,

$$|\psi_L\rangle=\sum_{[\boldsymbol{\xi}^L]}\prod_{i+j=even}A_L\begin{pmatrix}\boldsymbol{\sigma}_{ij}^L\\ \boldsymbol{\xi}_{ij}^L\end{pmatrix}, \tag{8}$$

where we assume that details of $|\psi_0\rangle$ can be ignored for sufficiently large L. Taking the limit $L\to\infty$, we obtain the maximum-eigenvalue eigenvector $|\psi_{\max}\rangle$, which is now represented as the product of the local tensor A_∞.

From the practical view point of the usual power method, the eigenvector is improved with the relation $|\psi_{L+1}\rangle$

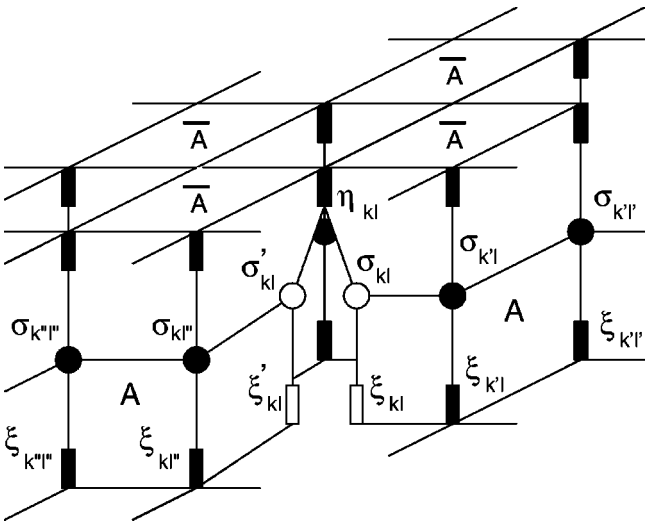

FIG. 3. The vertical density matrix $\rho_{kl}(\sigma'_{kl}\xi'_{kl}|\sigma_{kl}\xi_{kl})$.

$=T|\psi_L\rangle$ iteratively. In the framework of the TPS, this power method is reformulated as the recursion relation for the local tensor,

$$A_{L+1}\begin{pmatrix}\boldsymbol{\sigma}_{ij}^{L+1}\\ \boldsymbol{\xi}_{ij}^{L+1}\end{pmatrix}=W\begin{pmatrix}\boldsymbol{\sigma}_{ij}^{L+1}\\ \boldsymbol{\sigma}_{ij}^{L}\end{pmatrix}A_L\begin{pmatrix}\boldsymbol{\sigma}_{ij}^{L}\\ \boldsymbol{\xi}_{ij}^{L}\end{pmatrix}, \tag{9}$$

with which we can carry out the iterative calculation, until A_L gives a good approximation of A_∞. However it is generally difficult to store the tensor A_L in the computer memory for a sufficiently large L because the number of states of ξ_{ij}^L, which is denoted as M in the following, diverges exponentially as L increases.

In order to restrict the number of the auxiliary variable, we now import the idea of the DMRG into the TPS [1]. The essence of the DMRG is that the increased number of states for ξ_{ij}^{L+1} can be reduced, by using the ''projection operator'' generated from the ''density matrix.'' In the present case, the appropriate density matrix should be constructed for the spin variables $(\sigma_{ij}^L,\xi_{ij}^L)$ in the vertical direction (we thus call this density matrix ''the vertical density matrix'') [14]. Introducing the ''transposed'' local tensor,

$$\overline{A}\begin{pmatrix}\boldsymbol{\eta}_{ij}\\ \boldsymbol{\sigma}_{ij}\end{pmatrix}=W\begin{pmatrix}\overline{\boldsymbol{\sigma}}_{ij}^{0}\\ \overline{\boldsymbol{\sigma}}_{ij}^{1}\end{pmatrix}W\begin{pmatrix}\overline{\boldsymbol{\sigma}}_{ij}^{1}\\ \overline{\boldsymbol{\sigma}}_{ij}^{2}\end{pmatrix}\cdots W\begin{pmatrix}\overline{\boldsymbol{\sigma}}_{ij}^{L-1}\\ \boldsymbol{\sigma}_{ij}\end{pmatrix}, \tag{10}$$

the explicit form of the vertical density matrix is defined as (see Fig. 3),

$$\begin{aligned}\rho_{kl}(\sigma'_{kl}\xi'_{kl}|\sigma_{kl}\xi_{kl})=&\sum_{[\boldsymbol{\sigma}],[\boldsymbol{\xi}],[\boldsymbol{\eta}]}{}'\left[\prod_{i+j=even}{}'\overline{A}\begin{pmatrix}\boldsymbol{\eta}_{ij}\\ \boldsymbol{\sigma}_{ij}\end{pmatrix}A\begin{pmatrix}\boldsymbol{\sigma}_{ij}\\ \boldsymbol{\xi}_{ij}\end{pmatrix}\right]\\ &\times\overline{A}\begin{pmatrix}\boldsymbol{\eta}_{k''l''}\\ \check{\boldsymbol{\sigma}}_{k''l''}\end{pmatrix}A\begin{pmatrix}\check{\boldsymbol{\sigma}}_{k''l''}\\ \check{\boldsymbol{\xi}}_{k''l''}\end{pmatrix}\\ &\times\overline{A}\begin{pmatrix}\boldsymbol{\eta}_{kl}\\ \boldsymbol{\sigma}_{kl}\end{pmatrix}A\begin{pmatrix}\boldsymbol{\sigma}_{kl}\\ \boldsymbol{\xi}_{kl}\end{pmatrix},\end{aligned} \tag{11}$$

where Σ' denotes the configuration sum for the all spin variables except σ'_{kl}, ξ'_{kl}, σ_{kl}, and ξ_{kl}. Π' means the product for the site (i,j) except $(i,j)=(k,l)$ and $(k'',l'')\equiv(k-1,l-1)$. In Eq. (11), we have also used the notation for the ''checked spins'':

$$\begin{pmatrix}\check{\boldsymbol{\sigma}}_{k''l''}\\ \check{\boldsymbol{\xi}}_{k''l''}\end{pmatrix}\equiv\begin{pmatrix}\sigma_{k''l''} & \sigma_{kl''} & \sigma'_{kl} & \sigma_{k''l}\\ \xi_{k''l''} & \xi_{kl''} & \xi'_{kl} & \xi_{k''l}\end{pmatrix}.$$

Further, we have omitted the sub(super)script L as it is apparent.

For the case of the isotropic 3D Ising model, the vertical density matrix ρ_{kl} is independent of the site index kl in the thermodynamic limit. Thus we write ρ_{kl} simply as ρ here. Moreover it should be noted that, for the isotropic case, the local tensors A and $\overline{A}$ satisfies the relation

$$\overline{A}\begin{pmatrix}\eta_{ij} & \eta_{i'j} & \eta_{i'j'} & \eta_{ij'}\\ \sigma_{ij} & \sigma_{i'j} & \sigma_{i'j'} & \sigma_{ij'}\end{pmatrix}=A\begin{pmatrix}\sigma_{ij} & \sigma_{ij'} & \sigma_{i'j'} & \sigma_{i'j}\\ \eta_{ij} & \eta_{ij'} & \eta_{i'j'} & \eta_{i'j}\end{pmatrix}. \tag{12}$$

Following the spirit of the DMRG, we diagonalize ρ to have the eigenvalues $w_{\tilde{\xi}}$ in the decreasing order $w_1\geqslant w_2\geqslant\cdots\geqslant w_{2M}(\geqslant 0)$,

$$\sum_{\sigma\xi}\rho(\sigma'\xi'|\sigma\xi)U(\sigma\xi|\tilde{\xi})=U(\sigma'\xi'|\tilde{\xi})w_{\tilde{\xi}}, \tag{13}$$

where $U(\sigma\xi|\tilde{\xi})$ is the eigenvector for $w_{\tilde{\xi}}$. By taking $U(\sigma\xi|\tilde{\xi})$ with $\tilde{\xi}\in 1,\ldots,M$, we construct the projection operator U, which is a $2M\times M$ rectangular matrix. Operating U on the spin variables on each ''edge'' of A, we then make the renormalized local tensor $\tilde{A}$,

$$\begin{aligned}\tilde{A}\begin{pmatrix}\boldsymbol{\tau}_{ij}\\ \tilde{\boldsymbol{\xi}}_{ij}\end{pmatrix}\equiv&\sum_{\boldsymbol{\sigma}_{ij},\boldsymbol{\xi}_{ij}}W\begin{pmatrix}\tau_{ij} & \tau_{i'j} & \tau_{i'j'} & \tau_{ij'}\\ \sigma_{ij} & \sigma_{i'j} & \sigma_{i'j'} & \sigma_{ij'}\end{pmatrix}\\ &\times A\begin{pmatrix}\sigma_{ij} & \sigma_{i'j} & \sigma_{i'j'} & \sigma_{ij'}\\ \xi_{ij} & \xi_{i'j} & \xi_{i'j'} & \xi_{ij'}\end{pmatrix}U(\sigma_{ij}\xi_{ij}|\tilde{\xi}_{ij})\\ &\times U(\sigma_{i'j}\xi_{i'j}|\tilde{\xi}_{i'j})U(\sigma_{i'j'}\xi_{i'j'}|\tilde{\xi}_{i'j'})\\ &\times U(\sigma_{ij'}\xi_{ij'}|\tilde{\xi}_{ij'}).\end{aligned} \tag{14}$$

Using Eqs. (9) and (14) recursively, we can now calculate the effective local tensor $\tilde{A}_\infty$. However we encounter another problem in this process; it is also a numerically heavy problem to compute the vertical density matrix with Eq. (11), where a huge memory space to store the spin variables is required in carrying out the summation.

Let us next explain how to overcome the difficulty in calculating the vertical density matrix. The key idea is that we can consider Eq. (11) as a configuration sum for a kind of 2D classical spin system with a point defect. To see it, we define here a new tensor

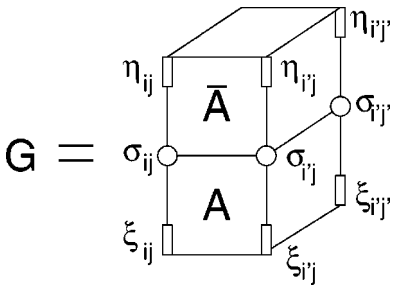

FIG. 4. The effective Boltzmann weight G.

$$G\begin{pmatrix}\boldsymbol{\eta}_{ij}\\ \boldsymbol{\sigma}_{ij}\\ \boldsymbol{\xi}_{ij}\end{pmatrix}\equiv\bar{A}\begin{pmatrix}\boldsymbol{\eta}_{ij}\\ \boldsymbol{\sigma}_{ij}\end{pmatrix}A\begin{pmatrix}\boldsymbol{\sigma}_{ij}\\ \boldsymbol{\xi}_{ij}\end{pmatrix}, \tag{15}$$

which is graphically represented in Fig. 4.

Regarding the spin variables along the z axis as a $2M^2$ state single spin,

$$s_{ij}=\begin{pmatrix}\eta_{ij}\\ \sigma_{ij}\\ \xi_{ij}\end{pmatrix}, \tag{16}$$

we can see that $G(\mathbf{s}_{ij})=G(s_{ij}s_{i'j}s_{i'j'}s_{ij'})$ becomes the Boltzmann weight for the 2D effective classical model. Then the vertical density matrix ρ can be expressed as the density matrix for the spin variables at the center of the 2D classical model,

$$\rho_{kl}(\sigma'_{kl}\xi'_{kl}|\sigma_{kl}\xi_{kl})=\sum'_{[\boldsymbol{\sigma}],[\boldsymbol{\xi}],[\boldsymbol{\eta}]}\left[\prod'_{i+j=even}G(\mathbf{s}_{ij})\right]\times G(\check{\mathbf{s}}_{k''l''})G(\mathbf{s}_{kl}) \tag{17}$$

where the meaning of the prime at the summation and the product is the same as Eq. (11), and the ''checked spin'' is given by

$$\check{\mathbf{s}}_{k''l''}=\begin{pmatrix}\boldsymbol{\eta}_{k''l''}\\ \check{\boldsymbol{\sigma}}_{k''l''}\\ \check{\boldsymbol{\xi}}_{k''l''}\end{pmatrix}.$$

We calculate each component of the vertical density matrix (17) as a partition function of the 2D classical system with the point defect that consists of the four fixed spins σ'_{kl}, ξ'_{kl}, σ_{kl}, and ξ_{kl} sitting at the center of the system. To this end we apply the corner transfer matrix renormalization group (CTMRG) [15], which is quite efficient for 2D classical statistical systems. Particularly we note that the CTMRG works well for a problem with a point defect.

Thus we have obtained a closed algorithm to calculate the local tensor A with Eqs. (9) and (14), assisted by the CTMRG for the 2D effective classical model. We summarize the numerical procedure as follows.

(a) For the free-boundary condition in the Z direction, define the initial local tensor A_1 as

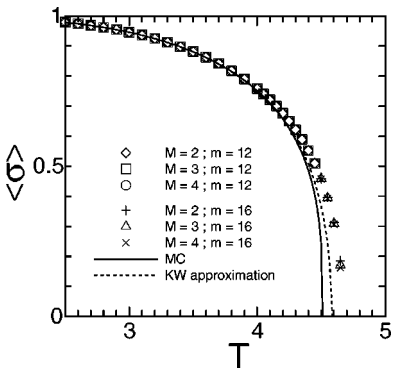

FIG. 5. The spontaneous magnetization of the 3D Ising model.

$$A_1\begin{pmatrix}\boldsymbol{\sigma}_{ij}\\ \boldsymbol{\sigma}'_{ij}\end{pmatrix}=W\begin{pmatrix}\boldsymbol{\sigma}_{ij}\\ \boldsymbol{\sigma}'_{ij}\end{pmatrix}. \tag{18}$$

For the Ferro boundary condition, define A_1 as

$$A_1\begin{pmatrix}\boldsymbol{\sigma}_{ij}\\ \boldsymbol{\sigma}'_{ij}\end{pmatrix}=W\begin{pmatrix}\boldsymbol{\sigma}_{ij}\\ \boldsymbol{\sigma}'_{ij}\end{pmatrix}\times W\begin{pmatrix}\boldsymbol{\sigma}'_{ij}\\ +1\end{pmatrix}, \tag{19}$$

where $(+1)$ means that the four Ising spins are aligned upward.

(b) Define the effective Boltzmann weight of the 2D classical spin system with Eq. (15).

(c) Perform the CTMRG calculation for the 2D effective classical spin system with the Boltzmann weight G and obtain the vertical density matrix ρ.

(d) Diagonalize ρ and construct the projection operator U.

(e) Renormalize the local tensor A with Eq. (14).

(f) Return to (b) until the local tensor A is converged.

In this VDMA calculation, the accuracy is determined by the number of retained basis M for the auxiliary variables ξ and η, and m for the CTMRG calculation in 2D classical system. We can check the convergence of the computed quantities with respect to M and m.

III. RESULTS

A. The 3D Ising model

Figure 5 shows the spontaneous magnetization $\langle\sigma\rangle$ calculated by using the VDMA. For comparison we also show the results of the 3D version of the Kramers-Wannier approximation [11] and Talapov and Blöte's Monte Carlo results [16]. After 20–50 iterations both in the vertical and horizontal directions, we have successfully reached the fixed point for each M and m. We find good convergence with respect to m in the whole temperature range and observe that the convergence with respect to M is also sufficient in the off-critical region. Near the critical point, however, the magnetization becomes smaller as M is increased, implying that large M is needed for the calculation in the critical region.

B. The 2D transverse field Ising model

Let us next consider the VDMA for the 2D transverse field Ising (TFI) model on the square lattice, which is one of

the fundamental quantum spin models in 2D. The Hamiltonian of the 2D TFI model is given by

$$H=-J\sum_{\langle i,j\rangle}\sigma_i^z\sigma_j^z-\Gamma\sum_i\sigma_i^x, \tag{20}$$

where $J(>0)$ is the ferromagnetic coupling constant, σ_i^α ($\alpha=x$, y, or z) are the Pauli matrices, and $\langle i,j\rangle$ denotes the nearest-neighbor pairs on the square lattice. The transverse field Γ induces the quantum fluctuation into the system. At zero temperature, the TFI model exhibits the quantum phase transition at $\Gamma=\Gamma_c$, below which the spontaneous magnetization $\langle\sigma\rangle$ behaves as $\langle\sigma\rangle\sim(\Gamma_c-\Gamma)^\beta$. The critical field Γ_c and the critical exponent β have been estimated as $\Gamma_c=3.06$ and $\beta=0.31$ by the quantum Monte Carlo (QMC) simulation [17]. In the following we consider the VDMA for the 2D TFI model at zero temperature and show the results of $\langle\sigma\rangle$.

As was described in the previous section, the VDMA is formulated for the 3D classical systems. In order to apply the VDMA to the 2D TFI model, we map the model to the 3D anisotropic Ising model by using the Suzuki-Trotter transformation [13]. The partition function Z of the 2D TFI model is obtained as the limit of the 3D anisotropic Ising model,

$$Z=\lim_{L\to\infty}\mathrm{Tr}\exp\left[K_h\sum_{\tau=1}^{L}\sum_{\langle i,j\rangle}\sigma_{i,\tau}\sigma_{j,\tau}+K_v\sum_{\tau=1}^{L}\sum_i\sigma_{i,\tau}\sigma_{i,\tau+1}\right], \tag{21}$$

where $\sigma_{i,\tau}$ is the Ising variable at the position i and imaginary time τ. The effective couplings K_h and K_v in Eq. (21) are given by

$$K_h=\epsilon J, \tag{22}$$

$$K_v=-\frac{1}{2}\ln[\tanh(\epsilon\Gamma)], \tag{23}$$

$$\epsilon=1/(TL), \tag{24}$$

where the subscripts h and v denote the horizontal (XY) direction and the vertical (Trotter) direction, respectively. We can perform the VDMA calculation for this anisotropic 3D Ising model.

We should make a comment on the boundary condition before proceeding to details. As was seen in the previous section, the open boundary condition is assumed in the VDMA. However, the periodic boundary condition is imposed along the Trotter direction in Eq. (21). As far as the zero-temperature properties are concerned, the boundary condition is inessential due to the double limit $T\to0$ and $L\to0$, allowing us to apply the VDMA to Eq. (21) [18].

For a fixed value of ϵ, we calculate the magnetization $\langle\sigma(\epsilon)\rangle$ with the VDMA for the infinite volume. After obtaining $\langle\sigma(\epsilon)\rangle$ for various ϵ, we take the $\epsilon\to0$ limit by extrapolation. In the actual calculation, we have observed the following ϵ dependence

$$\langle\sigma(\epsilon)\rangle=\langle\sigma(0)\rangle+\mathrm{const}\times\epsilon^2, \tag{25}$$

which we adopt as the extrapolation formula.

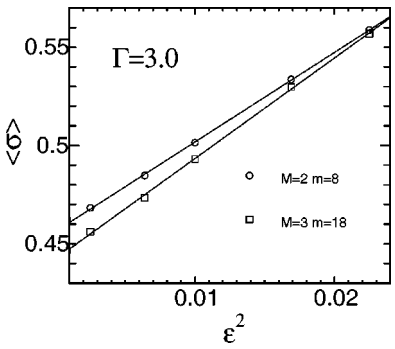

FIG. 6. The extrapolation of the magnetization at $\Gamma=3.0$. The solid lines are linear fits of data.

In Fig. 6, we show the $\langle\sigma\rangle$ vs ϵ^2 plots at $\Gamma=3.0$ as an example, which are obtained with the VDMA of the numbers of retained bases $(M,m)=(2,8)$ and $(3,18)$, where the convergence with respect to m is rapid. In the region $\Gamma>3.2$, $\langle\sigma\rangle$ converges to 0 smoothly.

In Fig. 7, we show the $\langle\sigma\rangle$-Γ curve and the results of the series expansion for comparison [19]. For $\Gamma<2.6$, the VDMA results are sufficiently reliable, where the number of the VDMA iterations is of the order of 10 in both Trotter and horizontal directions and the convergency about m and M is also good. In the small field region ($\Gamma<2.0$) then, we can see the good agreement of the VDMA results with the series expansion. In the vicinity of the critical point, however, the calculated magnetization exhibits M dependence. In addition, we note that several thousands of iterations are required in the Trotter direction, whereas at most 50 iterations are needed in the horizontal direction. The roughly estimated critical field from the VDMA calculation is about 3.2, which is 4% larger than the QMC one.

IV. CONCLUSION

In this paper we have constructed a higher-dimensional numerical renormalization algorithm that utilizes the natural tensor-product form of the maximum-eigenvalue eigenstate $|\psi_{\max}\rangle$ of the transfer matrix. In our algorithm, called

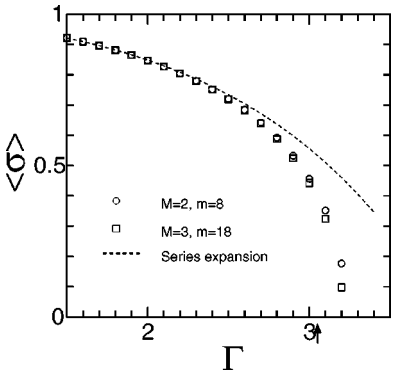

FIG. 7. $\epsilon=0$ limit of $\langle\sigma\rangle$-Γ curve at $T=0$. The arrow shows the critical field obtained by the QMC simulation [17].

VDMA, the local tensor forming $|\psi_{\max}\rangle$ is iteratively updated using the vertical density matrix. We have successfully applied the VDMA to the 3D Ising model. The VDMA can also be applied to 2D quantum systems using the Suzuki-Trotter transformation to 3D classical statistical systems, which we have demonstrated for the 2D transverse field Ising model. Application of the VDMA to other 2D quantum systems such as the Heisenberg model is an important subject of study, which we are now undertaking.

ACKNOWLEDGMENTS

Y.H. and K.O. were supported by the Japan Society for the Promotion of Science (JSPS). This work was partially supported by the ''Research for the Future'' program from the JSPS (Grant No. JSPS-RFTF97P00201) and by the Grant-in-Aid for Scientific Research from the Ministry of Education, Science, Sports and Culture (No. 12640393 and No. 11640376).

[1] S.R. White, Phys. Rev. Lett. **69**, 2863 (1992); Phys. Rev. B **48**, 10 345 (1993).

[2] *Density-Matrix Renormalization — A New Numerical Method in Physics*, edited by I. Peschel, X. Wang, M. Kaulke, and K. Hallberg, Lecture Notes in Physics Vol. 528 (Springer-Verlag, Berlin, 1999).

[3] S. Liang and H. Pang, Phys. Rev. B **49**, 9214 (1994); R. M. Noack, S. R. White, and D. J. Scalapino, in *Computer Simulations in Condensed Matter Physics VII*, edited by D. P. Landau, K. K. Mon, and H. B. Schüttler (Spinger-Verlag, Berlin, 1994).

[4] T. Nishino and K. Okunishi, J. Phys. Soc. Jpn. **67**, 3066 (1998).

[5] P. Henelius, Phys. Rev. B **60**, 9561 (1999).

[6] M.A. Martin-Delgado, J. Rodriguez-Laguna, and G. Sierra, Nucl. Phys. B **601**, 569 (2001).

[7] S. Östlund and S. Rommer, Phys. Rev. Lett. **75**, 3537 (1995); S. Rommer and S. Östlund, Phys. Rev. B **55**, 2164 (1997).

[8] I. Affleck, T. Kennedy, E.H. Lieb, and H. Tasaki, Phys. Rev. Lett. **59**, 799 (1987); I. Affleck, T. Kennedy, E.H. Lieb, and H. Tasaki, Commun. Math. Phys. **115**, 477 (1988); T. Kennedy, E.H. Lieb, and H. Tasaki, J. Stat. Phys. **53**, 383 (1988).

[9] Y. Hieida, K. Okunishi, and Y. Akutsu, New J. Phys. **1**, 7 (1999).

[10] H. Niggemann, A. Klümper, and J. Zittartz, Z. Phys. B: Condens. Matter **104**, 103 (1997); H. Niggemann, A. Klümper, and J. Zittartz, Eur. Phys. J. B **13**, 15 (2000).

[11] K. Okunishi and T. Nishino, Prog. Theor. Phys. **103**, 541 (2000).

[12] T. Nishino, K. Okunishi, Y. Hieida, N. Maeshima, and Y. Akutsu, Nucl. Phys. B **575**, 504 (2000); T. Nishino, Y. Hieida, K. Okunishi, N. Maeshima, Y. Akutsu, and A. Gendiar, Prog. Theor. Phys. **105**, 409 (2001).

[13] H.F. Trotter, Proc. Am. Math. Soc. **10**, 545 (1959); M. Suzuki, Prog. Theor. Phys. **56**, 1454 (1976).

[14] In Ref. [1] the superblock is constructed as $B\bullet\bullet B$, where B and $\bullet$ represent the block and the single site, respectively. In the VDMA algorithm, however, we construct the superblock as $B\bullet B_e$. B_e represents the environment block and $B \neq B_e$. In this case, the environment block B_e contains much more sites than the system block $B\bullet$ that corresponds to $(\sigma_{kl}\xi_{kl})$. For example, B_e contains $\eta_{kl}, \eta_{k+1l-1}, \eta_{k-1l+1}, \ldots$ (see Fig. 3).

[15] T. Nishino and K. Okunishi, J. Phys. Soc. Jpn. **65**, 891 (1996).

[16] A.L. Talapov and H.W.J. Blöte, J. Phys. A **29**, 5727 (1996).

[17] T. Ikegami, S. Miyashita, and H. Rieger, J. Phys. Soc. Jpn. **67**, 2671 (1998).

[18] M. Barma and B.S. Shastry, Phys. Rev. B **18**, 3351 (1978).

[19] P. Pfeuty and R.J. Elliott, J. Phys. C **4**, 2370 (1971).